Gene Expression **2025** vol. 24(4) | e00056
DOI: 10.14218/GE.2025.00056

Original Article

Gene–environment Interaction of GWAS Loci and Reproductive History in Uterine Fibroid Risk: A Case-control Study

Liubov Ponomareva[1,2], Ekaterina Barysheva[1], Anna Dorofeeva[1], Ksenia Kobzeva[1] and Olga Bushueva[1,3*]

[1]*Laboratory of Genomic Research, Research Institute for Genetic and Molecular Epidemiology, Kursk State Medical University, Kursk, Russia;* [2]*Department of Obstetrics and Gynecology, Institute of Continuing Education, Kursk State Medical University, Kursk, Russia;* [3]*Department of Biology, Medical Genetics and Ecology, Kursk State Medical University, Kursk, Russia*

Received: June 19, 2025 | **Revised:** July 22, 2025 | **Accepted:** August 14, 2025 | **Published online:** October 14, 2025

Abstract

Background and objectives: Uterine fibroids (UFs) are common hormone-dependent tumors with a complex etiology involving both genetic and environmental factors. This study aimed to investigate, for the first time, the associations between loci from genome-wide association studies (GWAS) and environmental risk factors in UF development, with a particular focus on gene–environment interactions.

Methods: DNA samples from 737 women with UF and 451 healthy controls were genotyped for ten UF-associated GWAS single nucleotide polymorphisms (SNPs) using probe-based polymerase chain reaction in this case-control study.

Results: SNP rs66998222 (*LOC102723323*, G/A) was associated with decreased UF risk in the total sample (odds ratio (OR) = 0.81, $p = 0.038$) and in patients with a history of induced abortion (OR = 0.70, $p = 0.009$). SNP rs11031731 (*THEM7P, WT1*, G/**A**) increased UF risk overall (OR = 1.39, $p = 0.01$), and in women with abortion history (OR = 1.60, $p = 0.008$) or without pelvic inflammatory disease (OR = 1.43, $p = 0.02$). SNPs rs641760 (*PITPNM2*, C/**T**) and rs2553772 (*LOC105376626*, G/**T**) showed protective effects depending on abortion history. SNP rs1986649 (*FOXO1*, C/**T**) was associated with later UF onset ($p = 0.049$) and slower growth ($p = 0.017$). GWAS loci influence UF-related genes involved in proliferation, inflammation, and hormone metabolism, underscoring their pathogenic role.

Conclusions: Induced abortions and inflammation modify the effects of GWAS-identified UF risk loci, with allele-specific impacts on hormonal, inflammatory, and repair pathways. Replication in diverse cohorts is needed to validate these population-specific effects.

Introduction

Uterine fibroids (UFs), or leiomyomas, are among the most common benign tumors of the female reproductive system, with prevalence rates reaching up to 68% among women of reproductive age.[1,2] This condition is often associated with symptoms such as heavy menstrual bleeding and pelvic pain, significantly affecting reproductive health and overall quality of life.[3] Although UFs affect a substantial proportion of women, the etiological pathways and mechanisms of disease progression remain incompletely understood, warranting further investigation into their pathogenic drivers.[4]

In recent years, genome-wide association studies (GWAS) have become an important tool for identifying single nucleotide polymorphisms (SNPs) associated with human diseases in general and with UF in particular.[5–10] These findings have significantly advanced our understanding of the molecular mechanisms underlying UF pathogenesis, paving the way for the development of

Keywords: Uterine fibroid; Inflammation; Abortion; Genome-wide association study; GWAS; rs66998222; rs11031731; rs641760; rs2553772.

***Correspondence to:** Olga Bushueva, Laboratory of Genomic Research, Research Institute for Genetic and Molecular Epidemiology, Kursk State Medical University, Kursk 305041, Russia. ORCID: https://orcid.org/0000-0003-3333-0623. Tel: +7-4712-588147, E-mail: olga.bushueva@inbox.ru

How to cite this article: Ponomareva L, Barysheva E, Dorofeeva A, Kobzeva K, Bushueva O. Gene–environment Interaction of GWAS Loci and Reproductive History in Uterine Fibroid Risk: A Case-control Study. *Gene Expr* 2025;24(4):e00056. doi: 10.14218/GE.2025.00056.

© 2025 The Author(s). This article has been published under the terms of Creative Commons Attribution-Noncommercial 4.0 International License (CC BY-NC 4.0), which permits noncommercial unrestricted use, distribution, and reproduction in any medium, provided that the following statement is provided. "This article has been published in *Gene Expression* at https://doi.org/10.14218/GE.2025.00056 and can also be viewed on the Journal's website at https://www.xiahepublishing.com/journal/ge".

targeted therapeutic approaches.[11] However, the interplay between GWAS-identified genetic loci and environmental risk factors remains insufficiently explored.

Environmental factors, including pelvic inflammatory disease (PID) and induced abortions, play a notable role in UF development and progression.[12–15] Growing interest in the interactions between genetic and environmental factors has highlighted the importance of examining their influences in a holistic context.[16,17] On one hand, SNPs identified through GWAS may predispose individuals to UF by modulating inflammatory, hormonal, and tissue-related processes.[18] On the other hand, environmental factors such as inflammation or myometrial trauma could amplify the activity of specific genetic loci, thereby modifying disease risk.[19] Previously, we examined GWAS loci associated with UF risk, selecting loci from the GWAS Catalog. That work was the first to demonstrate that these genetic associations could be modified by environmental factors such as smoking, intake of fresh vegetables and fruits, and reproductive risk factors.[19]

This study aimed to investigate the associations between newly selected GWAS loci and reproductive risk factors in the development of uterine UF, with a particular focus on how induced abortions and PID modulate the associations between these loci and UF risk, explored here for the first time. Our study examines how environmental factors interact with genetic risk, either strengthening or weakening the effects of GWAS-identified loci on disease susceptibility. In the future, these data will help identify key mechanisms of pathogenesis and potential targets for preventive and therapeutic interventions.

Materials and methods

Study participants

We analyzed the same Central Russian cohort (n = 1,188) as in our previous work,[19] consisting of 737 clinically confirmed UF patients and 451 healthy controls. The studies were conducted in accordance with the guidelines of the Declaration of Helsinki (as revised in 2024), local legislation, and institutional requirements. The Ethics Committee of Kursk State Medical University approved all procedures (Protocol №5, May 11, 2021), with written consent obtained from all participants. Inclusion required self-reported Russian ethnicity and Central Russian birth origin. Table 1 summarizes the baseline characteristics of the participants.

Case participants with ultrasound-verified UF were enrolled from 2021 to 2023 at two tertiary care facilities: the Perinatal Centre and Kursk City Maternity Hospital. The control cohort, comprising individuals with no signs of UFs on clinical or ultrasound evaluation, was assembled through systematic screening during preventive health visits at regional medical centers and occupational health settings.[20,21] Figure 1 presents a comprehensive flowchart detailing the participant selection process and applied research methodology.

Selection of environment-associated risk factors for UFs

The following environmental risk factors for UF development were analyzed:

1. *Medical (induced) abortions*: These procedures may contribute to UF development through mechanisms such as the absence of hormonal regulation typically seen in late pregnancy following early estrogen surges, tissue repair processes resembling keloid formation, and cytokine-mediated inflammation. Collectively, these processes activate genetic and signaling pathways that drive abnormal tissue growth and fibroid formation.[13,14]
2. *PID:* Disorders associated with trauma, infection, or inflammatory processes disrupt immune homeostasis by upregulating T-helper cytokines while suppressing regulatory T cell activity. This dysregulation promotes excessive fibrotic tissue formation and proliferation.[12]

Genes and polymorphisms selection

Genes and polymorphisms were selected using the online Reproductive System Knowledge Portal (RSKP), which aggregates data from meta-analyses of GWAS of reproductive diseases worldwide (https://reproductive.hugeamp.org/) with the search query “uterine fibroids”. SNPs with a minor allele frequency < 0.05 were excluded, as were those presenting technical challenges for allele-specific fluorescent probe genotyping due to low GC content, absence of GC clamps, or homopolymeric nucleotide repeats. A total of ten SNPs were included in the genotyping: rs2235529 (*WNT4)*, rs59760198 (*DNM3)*, rs10929757 (*GREB1)*, rs1812266 (*LOC105375949)*, rs9419958 (*STN1)*, rs11031731 (*THEM7P, WT1),* rs2553772 (*LOC105376626)*, rs641760 (*PITPNM2)*, rs1986649 (*FOXO1)*, and rs66998222 (*LOC102723323)*.

Genetic analysis

Genotyping was conducted at the Laboratory of Genomic Research, Research Institute for Genetic and Molecular Epidemiology, Kursk State Medical University (Kursk, Russia). Participants provided up to 5 mL of venous blood, collected in ethylenediaminetetraacetic acid (EDTA)-coated tubes and stored at –20°C until analysis. Genomic DNA was extracted using standard protocols, including phenol/chloroform extraction and ethanol precipitation, and its purity, quality, and concentration were assessed using a NanoDrop spectrophotometer (Thermo Fisher Scientific, Waltham, MA, USA).

SNP genotyping was conducted via allele-specific fluorescent probes using custom-developed polymerase chain reaction (PCR) protocols. Primers were designed using Primer3 software.[22] Real-time PCR was performed in a 25 µL reaction volume containing 1.5 U of Hot Start Taq DNA polymerase (Biolabmix, Novosibirsk, Russia), approximately 10 ng of template DNA, and the following reagent concentrations: 0.25 µM of each primer, 0.1 µM of each probe, 250 µM of each dNTP, and varying $MgCl_2$ concentrations (1.5 mM for rs66998222; 3 mM for rs10929757, rs9419958, rs1812266, rs1986649, rs2553772, and rs11031731; 3.5 mM for rs641760 and rs2235529; 4 mM for rs59760198). PCR buffer (1×) included 67 mM Tris-HCl (pH 8.8), 16.6 mM $(NH_4)_2SO_4$, and 0.01% Tween-20. The thermal cycling protocol consisted of an initial denaturation at 95°C for 10 m, followed by 39 cycles of 92°C for 30 s and annealing/elongation at various temperatures for 1 m (60°C for rs1812266; 61°C for rs9419958; 64°C for rs1986649, rs2553772, rs11031731, rs2235529, and rs59760198; 65°C for rs10929757 and rs641760; 66°C for rs66998222).

For quality control, 10% of samples underwent blinded duplicate genotyping, demonstrating >99% concordance. The rs9419958 (STN1) SNP, which deviated from Hardy–Weinberg equilibrium in controls, was re-genotyped and showed 100% concordance with initial results, confirming data reliability.

Data analysis methods

Statistical analyses were performed using STATISTICA software (version 13.3, Santa Clara, CA, USA). The normality of data distributions was evaluated with the Shapiro–Wilk test. As most quantitative variables deviated from normality, results are presented

Table 1. Baseline and clinical characteristics of the study cohort

Baseline characteristics of the study cohort		UF group (n = 737)	Control group (n = 451)	*p*-value
Age, Me [Q1; Q3]		48 [43; 52]	51 [43; 59]	**<0.001**
Smoking	Yes, N (%)	108 (14.7%)	44 (9.7%)	>0.05
	No, N (%)	629 (85.3%)	407 (90.3%)	
Low fruit/vegetable consumption	Yes, N (%)	603 (81.8%)	ND	–
	No, N (%)	134 (18.2%)	ND	
Infertility history	Yes, N (%)	8 (1.1%)	2 (0.4%)	>0.05
	No, N (%)	566 (76.8%)	376 (83.4%)	
	ND, N (%)	163 (22.1%)	73 (16.2%)	
Pelvic inflammatory diseases (PID)	Yes, N (%)	108 (14.6%)	61 (13.5%)	>0.05
	No, N (%)	464 (63.0%)	318 (70.5%)	
	ND, N (%)	165 (22.4%)	72 (16%)	
Family history of UFs	Yes, N (%)	205 (27.8%)	36 (8%)	**<0.01**
	No, N (%)	532 (72.2%)	415 (92%)	
	ND, N (%)	–	–	
Menarche age (years)	Me [Q1; Q3]	12 [12; 14]	13 [12; 14]	>0.05
Pregnancy history	Yes, N (%)	622 (84.4%)	401 (88.9%)	>0.05
	No, N (%)	29 (3.9%)	13 (2.9%)	
	ND, N (%)	86 (11.7%)	37 (8.2%)	
Gravidity (total pregnancies)	Me [Q1; Q3]	3 [2; 5]	3 [2; 4]	>0.05
Parity	Yes, N (%)	604 (81.9%)	394 (87.4%)	>0.05
	No, N (%)	44 (6%)	19 (4.2%)	
	ND, N (%)	89 (12.1%)	38 (8.4%)	
Number of deliveries	Me [Q1; Q3]	2 [1; 2]	2 [1; 2]	>0.05
Medical abortion history	Yes, N (%)	438 (59.4%)	225 (49.9%)	>0.05
	No, N (%)	201 (27.3%)	178 (39.5%)	
	ND, N (%)	98 (13.3%)	48 (10.6%)	
Medical abortion numbers	Me [Q1; Q3]	1 [0; 2]	1 [0; 2]	>0.05
Miscarriages in anamnesis	Yes, N (%)	133 (18%)	82 (18.2%)	>0.05
	No, N (%)	478 (64.9%)	318 (70.5%)	
	ND, N (%)	126 (17.1%)	51 (11.3%)	
Number of miscarriages	Me [Q1; Q3]	0 [0; 0]	0 [0; 0]	>0.05
Periods prolongation (>7 days)	Yes, N (%)	180 (24.4%)	83 (18.4%)	>0.05
	No, N (%)	442 (60%)	305 (67.6%)	
	ND, N (%)	115 (15.6%)	63 (14%)	
Periods regularity	Yes, N (%)	357 (48.4%)	200 (44.3%)	**<0.001**
	No, N (%)	159 (21.6%)	2 (0.5%)	
	ND, N (%)	221 (30%)	249 (55.2%)	
Dysmenorrhea	Yes, N (%)	227 (30.8%)	23 (5.1%)	**<0.001**
	No, N (%)	236 (32%)	179 (39.7%)	
	ND, N (%)	274 (37.2%)	249 (55.2%)	

(continued)

Table 1. *- (continued)*

Baseline characteristics of the study cohort		UF group (n = 737)	Control group (n = 451)	*p*-value
Menorrhagia (heavy menstrual bleeding)	Yes, N (%)	370 (50.2%)	36 (8%)	**<0.001**
	No, N (%)	144 (19.5 %)	166 (36.8%)	
	ND, N (%)	223 (30.3%)	249 (55.2%)	
Age at uterine fibroid diagnosis (years)	Me [Q1; Q3]	40 [36; 45]	–	–
Uterine dimensions at time of diagnosis (gestational week equivalents)	Me [Q1; Q3]	7 [6; 9]	–	–
Current uterine size (weeks of gestation)	Me [Q1; Q3]	9 [7; 12]	–	–
Growth of UFs (weeks of gestation/year)	Me [Q1; Q3]	0.33 [0; 0.76]	–	–

Values are presented as Me (median) with interquartile range (Q1–Q3). Bold formatting marks statistically significant comparisons ($p < 0.05$). ND, unavailable data; UF, uterine fibroid.

as medians with interquartile ranges. Continuous variables were analyzed using the Mann–Whitney nonparametric test, while categorical variables were evaluated using Pearson's χ^2 test, incorporating Yates' continuity correction when appropriate for small sample sizes.

Hardy–Weinberg equilibrium for genotype distributions was assessed using Fisher's exact test. The SNPStats web-based platform (https://www.snpstats.net) was used to perform logistic regression analyses examining potential correlations between genotype distributions and UF susceptibility. Analyses followed an additive genetic model and were adjusted for confounding factors, including age and family history of UFs. To account for the potential influence of risk factors on genetic associations, separate analyses were conducted for patients with and without exposure to these factors.

The model-based (MB) multifactor dimensionality reduction (MDR) method was applied to investigate combinations of genotypes at two, three, and four loci, assessing both gene–gene (G×G) interactions and interactions between genotypes and UF risk factors (gene–environment, G×E).[23] Risk factors such as medical abortions and PID were included in the G×E interaction analyses. Empirical *p*-values (p_{perm}) for each model were calculated using permutation testing with 1,000 iterations—the default procedure for simultaneously testing all potential interactions of a given complexity.[24] Associations with permutation-adjusted significance (*pperm* < 0.05) were considered statistically reliable. All regression models were adjusted for patient age and documented family history of UFs.

Statistical computations were conducted in R software (version 3.6.3, R Foundation for Statistical Computing, Vienna, Austria). For each level of interaction, three to four models with the highest Wald statistics and most significant *p*-values were included in the final analysis. The MB-MDR method also allowed the identification of specific genotype combinations significantly associated with the studied phenotypes ($p < 0.05$). Analyses were performed using the MB-MDR program compatible with the R software (version 3.6.3).

To investigate the functional implications of the studied SNPs, several bioinformatics tools were utilized (described in detail in our previous research[25–27]):

- GTEx Portal (http://www.gtexportal.org/) was used to analyze SNP associations with expression quantitative trait loci (eQTLs) across various tissues, including reproductive organs, adipose tissue, blood, and endocrine glands.
- eQTLGen (https://www.eqtlgen.org/) provided additional insights into SNP–eQTL relationships, particularly in peripheral blood samples.
- HaploReg v4.2 (https://pubs.broadinstitute.org/mammals/haploreg/haploreg.php) was used to assess SNP positioning in regulatory elements, including DNase hypersensitive regions and histone modifications.
- atSNP Function Prediction (http://atsnp.biostat.wisc.edu/search) evaluated how SNP variants affected transcription factor (TF) binding affinity based on reference and alternative alleles.
- Gene Ontology (http://geneontology.org/) was used to identify biological processes enriched among TFs associated with the studied SNPs, linking these processes to UF pathogenesis.
- RSKP (https://cd.hugeamp.org/) integrated findings from genetic association studies, providing additional data on potential relationships between identified SNPs and UF-related clinical manifestations, including abnormal heavy menstrual bleeding and elevated body mass index (BMI).

Results

Association of GWAS loci with UF risk in Russian women

The distribution of SNP genotypes across study cohorts is presented in Table S1. As genetic associations may influence population equilibrium patterns, we first verified Hardy–Weinberg equilibrium in control subjects. All examined polymorphisms conformed to Hardy–Weinberg equilibrium expectations ($p > 0.05$), with the exception of rs9419958 in the *STN1* gene (Table S1). Technical validation through replicate genotyping confirmed 100% concordance for rs9419958, warranting its inclusion in subsequent analyses.

Association analysis revealed statistically significant relationships with UF risk (Table 2). The A allele of rs66998222 (*LOC102723323*) demonstrated a protective effect (odds ratio (OR) = 0.81, 95% confidence interval (CI) = 0.66–0.99, $p = 0.038$). Conversely, rs11031731 (*THEM7P, WT1*) was associated with increased disease susceptibility (effect allele A, OR = 1.39, 95% CI = 1.08–1.80, $p = 0.01$).

Gene-gene interactions analysis (MB-MDR, MDR modeling)

Using the MB-MDR approach, we identified eight significant gene–gene interaction models involving GWAS-identified loci associated with UF: four two-locus models, two three-locus models, and two four-locus models ($p_{perm} \leq 0.05$) (Table 3). Notably, five polymorphic loci, rs9419958 *(STN1)*, rs10929757 (*GREB1*), rs66998222 (*LOC102723323*), rs2553772 (*LOC105376626*), and

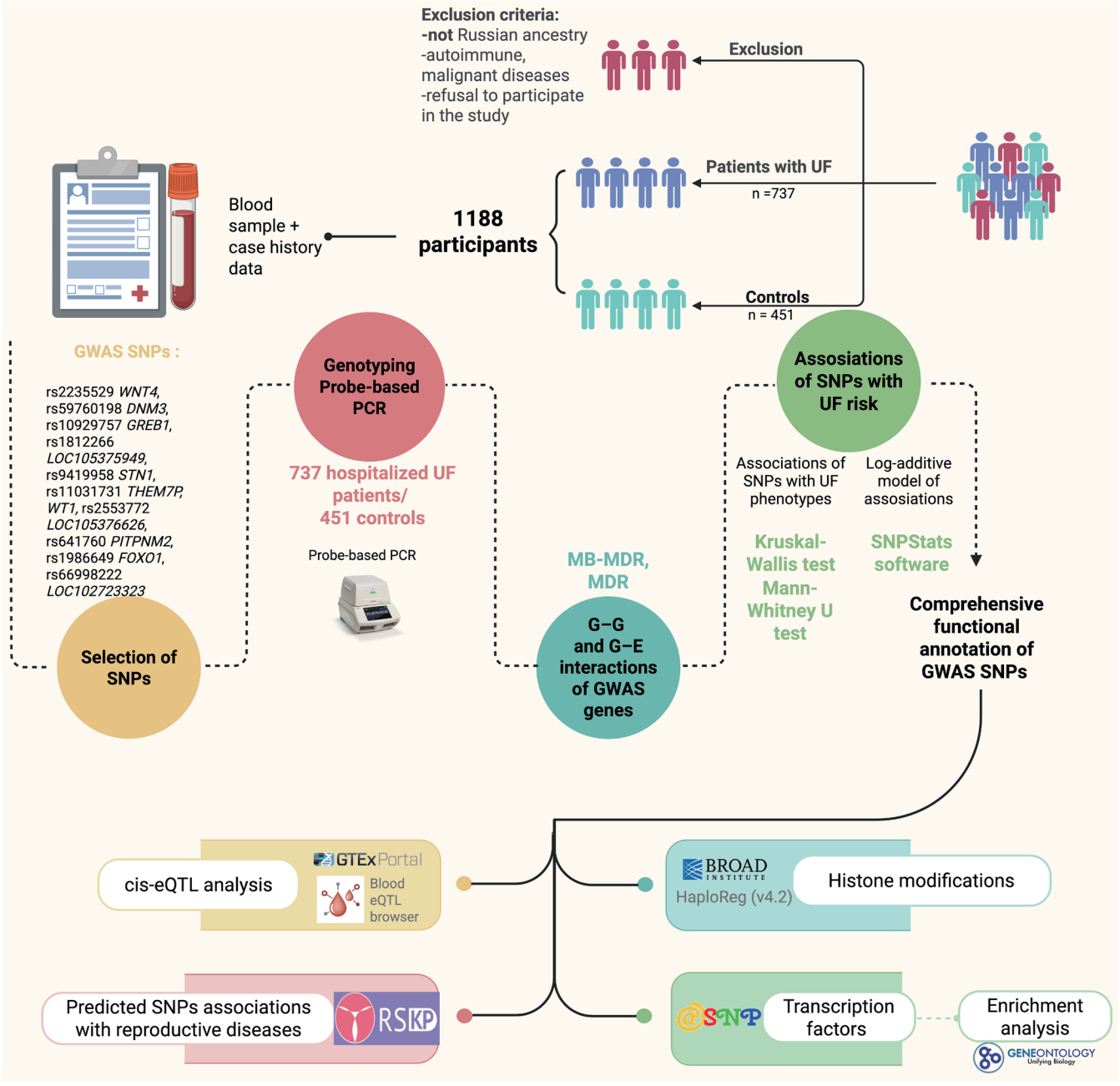

Fig. 1. Participant selection algorithm and methodological workflow. The participant flow diagram follows STROBE recommendations, documenting screening eligibility, exclusions, final analytical sample composition, and applied research methodology. eQTL, expression quantitative trait loci; GWAS, genome-wide association studies; MB, Model-Based; MDR, Multifactor Dimensionality Reduction; PCR, Polymerase chain reaction; SNP, single nucleotide polymorphism; STROBE, Strengthening of Reporting of Observational Studies in Epidemiology; UF, uterine fibroid.

rs2235529 (*WNT4*), were incorporated into two or more of the most statistically significant gene–gene interaction patterns, suggesting their potential role in polygenic disease mechanisms. At the next stage, the interactions of these genetic variants were analyzed using the MDR method (Fig. 2).

The MDR method indicated that the genetic variants included in the best G×G models exhibited multidirectional effects (synergism, antagonism, and additive effects). Alongside interaction analyses, we separately evaluated the individual (mono) effects of the genetic variants comprising the most significant gene–gene interaction models. Their contributions to UF entropy (0.02–0.39%) were comparable with the effects of intergenic interactions (0.01%–0.42%). The most pronounced mono-effect was observed for rs9419958 (*STN1*; 0.39% entropy), while the strongest interactions occurred between rs2235529 (*WNT4*) and rs2553772 (*LOC105376626*; 0.42% entropy; pronounced synergism). Among the strongest associations with UF risk were specific genotype combinations from interacting polymorphic variants, revealing al-

Table 2. Results of the analysis of associations between GWAS SNPs and UFs in the entire group

Genetic variant	Effect allele	Other allele	N	OR [95% CI][a]	*p*[b]
Entire group					
rs66998222 *LOC102723323*	A	G	1056	**0.81 [0.66–0.99]**	**0.038**
rs641760 *PITPNM2*	T	C	1050	0.81 [0.65–1.01]	0.06
rs2553772 *LOC105376626*	T	G	1052	0.87 [0.73–1.04]	0.13
rs10929757 *GREB1*	A	C	1054	0.97 [0.81–1.16]	0.71
rs2235529 *WNT4*	T	C	1047	1.06 [0.82–1.36]	0.67
rs59760198 *DNM3*	T	C	1037	1.10 [0.91–1.32]	0.32
rs1812266 *LOC105375949*	C	G	1056	1.12 [0.93–1.33]	0.23
rs1986649 *FOXO1*	T	C	1055	1.12 [0.89–1.40]	0.33
rs9419958 *STN1*	T	C	1056	1.26 [1.00–1.60]	0.05
rs11031731 *THEM7P, WT1*	A	G	1056	**1.39 [1.08–1.80]**	**0.01**

All statistical models used the minor allele as the reference and controlled for age and familial UF history. Data show: [a]adjusted odds ratios with 95% CIs; [b]significance values. Bold indicates $p < 0.05$. CI, confidence interval; GWAS, genome-wide association studies; OR, odds ratio; SNP, single nucleotide polymorphism; UF, uterine fibroid.

lelic patterns that may influence disease susceptibility: 1) Decrease risk of UF: rs9419958 *STN1* C/C × rs10929757 *GREB1* C/A (beta = −0.08, $p = 0.01$), rs641760 *PITPNM2* C/T × rs9419958 *STN1* C/C (beta = −0.087, $p = 0.01$), rs9419958 *STN1* C/C × rs66998222 *LOC102723323* A/G (beta = −0.11, $p = 0.002$), rs9419958 *STN1* C/C × rs59760198 *DNM3* C/C × rs66998222 *LOC102723323* A/G (beta = −0.198, $p = 0.001$), rs11031731 *THEM7P, WT1* G/G × rs9419958 *STN1* C/C × rs10929757 *GREB1* C/A × rs66998222 *LOC102723323* A/A (beta = −0.45, $p = 0.0001$), rs2553772 *LOC105376626* T/G × rs2235529 *WNT4* T/C × rs10929757 *GREB1* C/C × rs66998222 *LOC102723323* A/G (beta = −0.557, $p = 0.003$); 2) Increase disease risk: rs2553772 T/T × rs9419958 T/C (beta = 0.186, $p = 0.006$), rs2553772 *LOC105376626* T/T × rs2235529 *WNT4* C/C × rs9419958 *STN1* T/C (beta = 0.29, $p = 0.001$) (Table S2).

Environmental risk factor stratification analysis of GWAS SNPs

The investigation extended to interactions with environmental risk factors, with detailed stratified analyses presented in Table S3 and summarized in Table 4. We found that rs66998222 (*LOC102723323*; OR = 0.70, 95% CI = 0.54–0.91, $p = 0.009$) and rs641760 (*PITPNM2*; OR = 0.71, 95% CI = 0.53–0.96, $p = 0.026$) were associated with a reduced risk of UF in patients with a history of induced abortions. Stratified analysis revealed that rs2553772

Table 3. UF-associated gene-gene interactions (MB-MDR modeling)

Gene-gene interaction models	NH	βH	WH	NL	βL	WL	Wmax	p_{perm}
The best two-locus models of intergenic interactions (for G×G models with $p_{min} < 0.002$, 1000 permutations)								
rs9419958 *STN1* × **rs10929757** *GREB1*	2	0.1434	10.253	1	−0.0800	6.156	10.253	0.028
rs641760 *PITPNM2* × **rs9419958** *STN1*	1	0.0730	3.121	2	−0.1064	10.030	10.030	0.029
rs2553772 *LOC105376626* × **rs9419958** *STN1*	2	0.1433	10.110	1	−0.1226	8.554	10.110	0.033
rs9419958 *STN1* × **rs66998222** *LOC102723323*	1	0.1158	4.637	1	−0.1108	9.856	9.856	0.033
The best three-locus models of intergenic interactions (for G×G models with $p_{min} < 1\times10^{-4}$, 1000 permutations)								
rs2553772 *LOC105376626* × **rs2235529** *WNT4* × **rs9419958** *STN1*	4	0.2192	20.519	4	−0.1415	8.741	20.52	0.002
rs9419958 *STN1* × rs59760198 *DNM3* × **rs66998222** *LOC102723323*	0	NA	NA	4	−0.1652	22.016	22.02	0.006
The best four-locus models of gene-gene interactions (for G×G models with $p_{min} < 1\times10^{-8}$, 1000 permutations)								
rs11031731 *THEM7P, WT1* × **rs9419958** *STN1* × **rs10929757** *GREB1* × **rs66998222** *LOC102723323*	2	0.1961	6.218	6	−0.2643	41.58	41.58	< 0.001
rs2553772 *LOC105376626* × **rs2235529** *WNT4* × **rs10929757** *GREB1* × **rs66998222** *LOC102723323*	4	0.1868	17.256	8	−0.4425	40.01	40.01	0.001

All models control for age and familial UF history. Loci participating in multiple optimal G×G models are bolded. MB, Model-Based; MDR, Multifactor Dimensionality Reduction; NH, number of high-risk genotype interactions; NL, low-risk interaction count; p_{perm}, permutation-adjusted *p*-value; UF, uterine fibroid; WH, high-risk Wald statistic; WL, low-risk Wald statistic; βH, high-risk interaction coefficient; βL, low-risk coefficient.

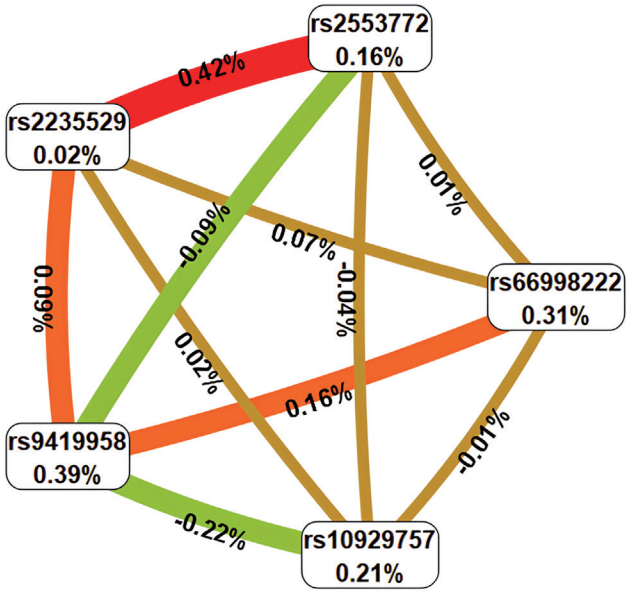

Fig. 2. Architecture of significant epistatic G×G networks in UF pathogenesis. Color coding: red/orange = synergistic; green = antagonistic; brown = additive interactions. Line thickness scales with effect magnitude (% entropy contribution). UF, uterine fibroid.

(*LOC105376626*) conferred protection against UF specifically in women without a history of induced abortion (OR = 0.61, 95% CI = 0.45–0.82, p = 0.001). Conversely, rs11031731 (*THEM7P/WT1*) showed risk-enhancing effects both in women with a history of abortion (OR = 1.60, 95% CI = 1.12–2.28, p = 0.008) and in those without a history of PID (OR = 1.43, 95% CI = 1.04–1.96, p = 0.02).

Gene-environment interactions of UF GWAS genes (MB-MDR, MDR modeling)

MB-MDR analysis identified five significant gene-environment interaction models: two two-level, two three-level, and one four-level interaction (Table 5). Remarkably, SNPs rs2553772 (*LOC105376626*) and rs1986649 (*FOXO1*), along with induced abortions, participated in two or more of the best gene–environment interaction models, and the interaction of induced abortions × rs2553772 (*LOC105376626*) contributed to three of these five top G×E interactions. At the next stage, the interactions of these genetic variants and risk factors were analyzed using the MDR method (Fig. 3).

First, the MDR methodology quantified induced abortions as having the strongest individual environmental effect (1.15% entropy contribution), exceeding both individual SNP effects (0.11–0.16%) and G×E interaction effects (0.05–0.34%). Second, induced abortions were characterized by pronounced synergism in interaction with rs2553772 (*LOC105376626*) and additive (independent) effects in interaction with rs1986649 (*FOXO1*). Third, SNPs characterizing the best G×E models (rs2553772 *LOC105376626* and rs1986649 *FOXO1*) exhibited moderate antagonism in interaction with each other. Fourth, the following gene–environment interactions showed the strongest associations with reduced UF risk: no induced abortions × rs2553772 *LOC105376626* T/T (beta = −0.236, $p = 5.54\times10^{-5}$), no induced abortions × rs11031731 *THEM7P, WT1* G/G × rs1986649 *FOXO1* C/C (beta = −0.222, $p = 4.59\times10^{-8}$), no induced abortions × rs2553772 *LOC105376626* T/T × rs1812266 *LOC105375949* C/G (beta = −0.345, $p = 3.21\times10^{-5}$), induced abortions × rs2553772 *LOC105376626* G/G× rs59760198 *DNM3* C/C × rs66998222 *LOC102723323* A/G (beta = −0.21, p = 0.016). The following G×E interaction was most strongly associated with increased UF risk: induced abortions × rs1986649 *FOXO1* C/C (beta = 0.095, $p = 2.33\times10^{-3}$) (Table S4).

GWAS loci associated with clinical course parameters of UFs

We also assessed the influence of genotype associations on the quantitative characteristics of the UF clinical course (Fig. 4, Table S5). A pronounced association was observed for rs1986649 (*FOXO1*) with age of disease onset (p = 0.049) and UF growth rate (p = 0.017), so this SNP was included in further study.

Functional annotation of SNPs

QTL effects

According to the GTEx Portal, the C allele of SNP rs641760 (*PITPNM2*) is associated with increased expression of *CDK2AP1* in subcutaneous adipose tissue and whole blood, *RP11-282O18.3* in the uterus and subcutaneous adipose tissue, *C12orf65* in subcutaneous adipose tissue, and *ARL6IP4* in whole blood (Table 6). Conversely, this allele is linked to decreased expression of *KMT5A* and *ABCB9* in whole blood.

The eQTLGen Browser reports that the T allele of SNP rs641760 (*PITPNM2*) increases the expression of *SETD8*, *MPHOSPH9*, *PITPNM2*, *SNRNP35*, *OGFOD2*, and *EIF2B1*, while decreasing expression of *SBNO1* in blood (Table 6).

For SNP rs2553772 (*LOC105376626*), the G allele increases *CD44* expression in adipose tissue, while the T allele decreases *RP1-68D18.4* expression (Table 6).

Table 4. Effect modification by prior induced abortions and PID history on GWAS SNP–UF risk associations

SNP	Effect allele	Other allele	N	OR [95% CI]	p	N	OR [95% CI][a]	p[b]
			Without induced abortions			Induced abortions		
rs2553772 *LOC105376626*	T	G	331	**0.61 (0.45–0.82)**	**0.001**	585	1.04 (0.82–1.32)	0.75
rs66998222 *LOC102723323*	A	G	335	0.93 (0.65–1.33)	0.69	585	**0.70 (0.54–0.91)**	**0.009**
rs641760 *PITPNM2*	T	C	329	1.04 (0.72–1.49)	0.84	585	**0.71 (0.53–0.96)**	**0.026**
rs11031731 *THEM7P, WT1*	A	G	335	1.27 (0.80–2.01)	0.3	585	**1.60 (1.12–2.28)**	**0.008**
			Without PID			With PID		
rs11031731 *THEM7P, WT1*	A	G	696	**1.43 (1.04–1.96)**	**0.02**	136	2.01 (0.91–4.43)	0.07

All calculations were performed relative to the minor alleles (effect allele). [a]odds ratio and 95% confidence interval; [b]p-value; statistically significant differences are marked in bold. CI, confidence interval; GWAS, genome-wide association studies; OR, odds ratio; PID, pelvic inflammatory disease; SNP, single nucleotide polymorphism; UF, uterine fibroid.

Table 5. UF-associated gene–environment interactions (MB-MDR modeling)

Gene-environment interaction models	NH	βH	WH	NL	βL	WL	Wmax	p_{perm}
The best two-order models of gene-smoking interactions (for G×E models with $p_{min} < 1\times10^{-5}$, 1000 permutations)								
Ind_abort × **rs2553772** ***LOC105376626***	1	0.0597	3.265	2	–0.1653	21.60	21.60	< 0.001
Ind_abort × **rs1986649** ***FOXO1***	1	0.0950	9.321	1	–0.1671	21.48	21.48	< 0.001
The best three-order models of gene-interactions (for G×E models with $p_{min} < 1\times10^{-6}$, 1000 permutations)								
Ind_abort × rs11031731 *THEM7P, WT1* × **rs1986649** ***FOXO1***	3	0.0921	7.449	1	–0.222	30.39	30.39	< 0.001
Ind_abort × **rs2553772** **LOC105376626** × rs1812266 *LOC105375949*	1	0.1230	5.179	3	–0.245	26.31	26.31	0.002
The best four-order models of gene-interactions (for G×E models with $p_{min} < 1\times10^{-9}$, 1000 permutations)								
Ind_abort × **rs2553772** **LOC105376626** × rs59760198 *DNM3* × rs66998222 *LOC102723323*	5	0.1649	17.794	10	–0.2872	40.14	40.14	< 0.001

All models control for age and familial UF history. Loci participating in multiple optimal G×E models are bolded. Ind_abort, induced abortions; MB, model-based; MDR, multifactor dimensionality reduction; NH, number of high-risk genotype interactions; NL, low-risk interaction count; p_{perm}, permutation-adjusted *p*-value; UF, uterine fibroid; WH, high-risk Wald statistic; WL, low-risk Wald statistic; βH, high-risk interaction coefficient; βL, low-risk coefficient.

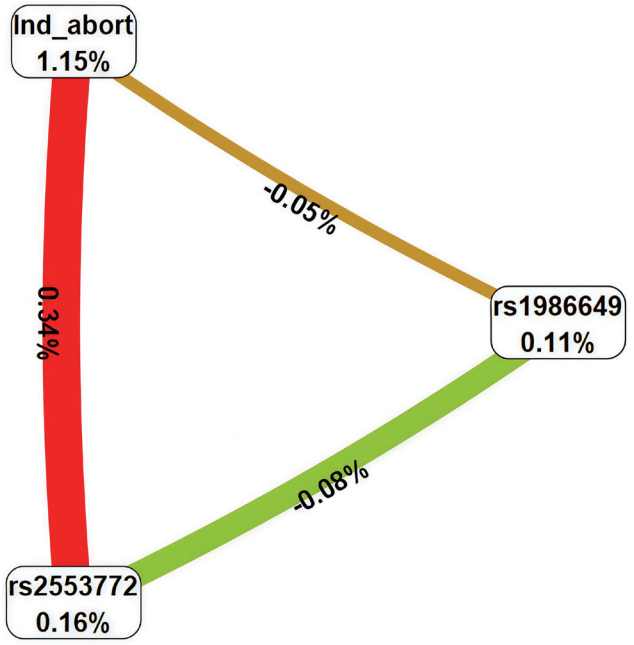

Fig. 3. Architecture of significant G×E interactions in UF pathogenesis. Key: Ind_abort, induced abortions; red: synergistic, green: antagonistic, brown: additive effects. Line thickness corresponds to the effect size (% entropy contribution). UF, uterine fibroid.

Finally, the T allele of SNP rs1986649 (*FOXO1*) correlates with increased *FOXO1* expression and decreased levels of *MRPS31*, *SLC25A15*, *ELF1*, *MIR621*, and *KBTBD7* in blood, as well as reduced *RLIMP1* expression in subcutaneous adipose tissue (Table 6).

Transcription factors

Analysis of TFs revealed that the risk allele A of rs66998222 (*LOC102723323*) creates DNA binding sites for 28 TFs, co-regulating negative regulation of cell population proliferation (GO:0008285; false discovery rate (FDR) = 0.0099) and cellular response to cytokine stimulus (GO:0071345; FDR = 0.0107). The protective allele G of rs66998222 (*LOC102723323*) creates DNA binding sites for 24 TFs, co-regulating interleukin (IL)-1 beta production (GO:0032651; FDR = 0.0229), response to hypoxia (GO:0001666; FDR = 0.0302), and positive regulation of cytokine production (GO:0001819; FDR = 0.0190) (Table S6).

The risk allele A of rs11031731 (*THEM7P, WT1*) generates DNA binding sites for 33 TFs involved in the regulation of adipose tissue development (GO:1904177; FDR = 0.0318) and cell population proliferation (GO:0008283; FDR = 0.0478). The protective allele G of rs11031731 (*THEM7P, WT1*) creates DNA binding sites for 35 TFs, regulating the following biological processes: regulation of cellular response to growth factor stimulus (GO:0090287; FDR = 0.0457), negative regulation of cell population proliferation (GO:0008285; FDR = 0.0230), positive regulation of apoptotic process (GO:0043065; FDR = 0.0311), negative regulation of cell differentiation (GO:0045596; FDR = 0.0130), and regulation of growth (GO:0040008; FDR = 0.0495) (Table S7).

The risk allele G of rs2553772 (*LOC105376626*) creates DNA binding sites for 20 TFs, jointly involved in the SREBP signaling pathway (GO:0032933; FDR = 0.0045), cellular response to transforming growth factor beta stimulus (GO:0071560; FDR = 0.0301), steroid metabolic process (GO:0008202; FDR = 0.0091), and nega-

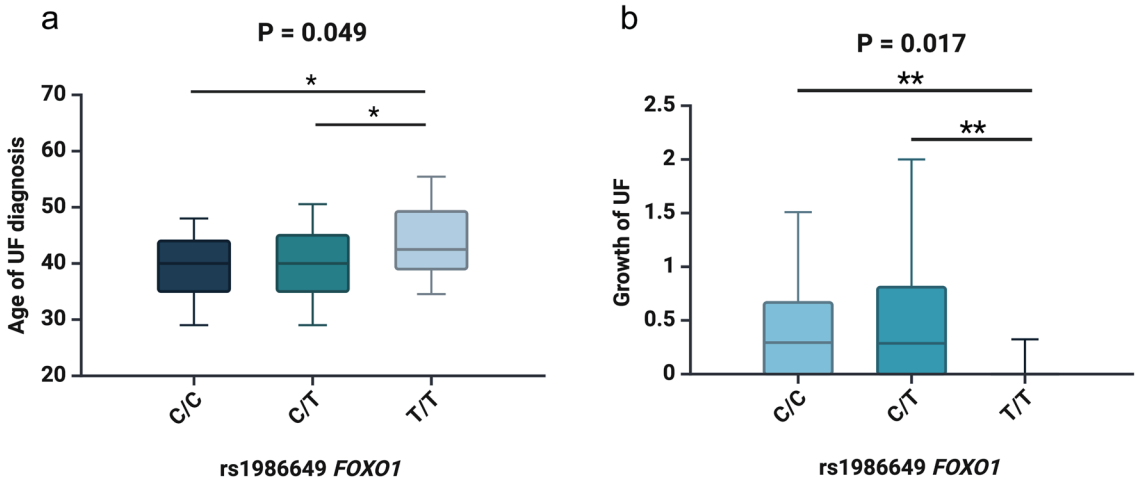

Fig. 4. Boxplots for statistically significant associations of GWAS SNP genotypes with clinical and biological characteristics of UF patients. (a) Age of UF diagnosis for rs1986649 FOXO1; (b) Growth of UFs (weeks of gestation/year) for rs1986649 FOXO1. UF, uterine fibroid; GWAS, genome-wide association studies; SNP, single nucleotide polymorphism.

tive regulation of cell population proliferation (GO:0008285; FDR = 0.0037). The protective allele T of rs2553772 (*LOC105376626*) generates DNA binding sites for 42 TFs, regulating the following biological processes: positive regulation of vascular endothelial growth factor production (GO:0010575; FDR = 0.0419), positive regulation of angiogenesis (GO:0045766; FDR = 0.0063), angiogenesis (GO:0001525; FDR = 0.0008), muscle organ development (GO:0007515; FDR = 0.0436), and regulation of cell population proliferation (GO:0042127; FDR = 0.0175) (Table S8).

The T allele of rs1986649 (*FOXO1*) creates DNA binding sites for 30 TFs, jointly involved in the SREBP signaling pathway (GO:0032933; FDR = 0.0067), positive regulation of transforming growth factor beta production (GO:0071636; FDR = 0.0206), regulation of IL-5 production (GO:0032674; FDR = 0.0239), SMAD protein signal transduction (GO:0060395; FDR = 0.0340), positive regulation of IL-4 production (GO:0032753; FDR = 0.0380),

Table 6. Cis-eQTL–mediated gene expression modulation by UF-linked GWAS SNPs (GTEx Portal and eQTLGen data)

Genetic variant	Assessed allele	Expressed gene	*p*	Effect (NES)	Tissue	Assessed allele	Symbol	Z-score	FDR
		GTEx portal					eQTLgene		
rs641760 *PITPNM2* (T/C)	C	*CDK2AP1*	2.3×10^{-32}	↑(0.40)	Adipose - Subcutaneous	T	*SETD8*	↑(21.4017)	0
		C12orf65	5.0×10^{-12}	↑(0.25)	Adipose - Subcutaneous		*MPHOSPH9*	↑(15.2575)	0
		RP11-282O18.3	3.2×10^{-7}	↑(0.22)	Adipose - Subcutaneous		*SBNO1*	↓(−8.2818)	0
		RP11-282O18.3	2.4×10^{-5}	↑(0.57)	Uterus		*PITPNM2*	↑(6.0034)	2×10^{-5}
		CDK2AP1	8.1×10^{-12}	↑(0.29)	Whole blood		*SNRNP35*	↑(5.9739)	2.6×10^{-5}
		KMT5A	1.9×10^{-9}	↓(−0.19)	Whole blood		*OGFOD2*	↑(5.3297)	0.0003
		ARL6IP4	3.4×10^{-5}	↑(0.072)	Whole blood		*EIF2B1*	↑(4.9115)	0.0026
		ABCB9	4.2×10^{-5}	↓(−0.13)	Whole blood				
rs2553772 *LOC105376626* (T/G)	G	*CD44*	8.8×10^{-8}	↑(0.13)	Adipose - Subcutaneous	T	*RP1-68D18.4*	↓(−5.2045)	0.0006
rs1986649 *FOXO1* (C/T)	T	*RLIMP1*	0.0001	↑(0.24)	Adipose - Subcutaneous	T	*MRPS31*		0
							FOXO1	↑(6.7807)	0
							SLC25A15	↓(−5.9359)	2.6×10^{-5}
							ELF1	↓(−4.8444)	0.0036
							MIR621	↓(−4.6621)	0.0083
							KBTBD7	↓(−4.3822)	0.0304

↑/↓, the effect on expression (increase or decrease). eQTL, expression quantitative trait loci; FDR, false discovery rate; GWAS, genome-wide association studies; NES, normalized effect size; SNP, single nucleotide polymorphism; UF, uterine fibroid.

Table 7. The impact of UF-associated GWAS SNPs on histone marks in various tissues

SNP (Ref/Alt allele)	Tissue marks	Blood	Blood vessels	Ovary	Adipose
rs66998222 *LOC102723323* (G/**A**)	H3K4me1	–	–	–	–
	H3K4me3	–	–	–	–
	H3K27ac	–	–	–	–
	H3K9ac	–	–	–	–
rs11031731 *THEM7P, WT1* (G/**A**)	H3K4me1	Enh	–	Enh	–
	H3K4me3	–	–	–	–
	H3K27ac	–	–	–	–
	H3K9ac	Pro	–	–	–
rs641760 *PITPNM2* (T/**C**)	H3K4me1	Enh	–	–	Enh
	H3K4me3	Pro	–	–	–
	H3K27ac	Enh	–	–	Enh
	H3K9ac	Pro	–	–	Pro
rs2553772 *LOC105376626* (T/**G**)	H3K4me1	Enh	Enh	–	Enh
	H3K4me3	Pro	–	–	–
	H3K27ac	Enh	–	–	Enh
	H3K9ac	Pro	–	–	–
rs1986649 *FOXO1* (C/**T**)	H3K4me1	Enh	–	Enh	Enh
	H3K4me3	Pro	–	–	–
	H3K27ac	Enh	–	–	Enh
	H3K9ac	–	–	–	Pro

Effect alleles are marked in bold. Enh, histone modification in the enhancer region; GWAS, genome-wide association studies; H3K27ac, acetylation at the 27th lysine residue of histone H3 protein; H3K4me1, mono-methylation at the 4th lysine residue of the histone H3 protein; H3K4me3, tri-methylation at the 4th lysine residue of the histone H3 protein; H3K9ac, the acetylation at the 9th lysine residue of the histone H3 protein; Pro, histone modification at the promoter region; SNP, single nucleotide polymorphism; UF, uterine fibroid.

cellular response to transforming growth factor beta stimulus (GO:0071560; FDR = 0.0042), and regulation of transforming growth factor beta receptor signaling pathway (GO:0017015; FDR = 0.0427). The reference allele C of rs1986649 (*FOXO1*) creates DNA binding sites for 57 TFs, co-regulating positive regulation of vitamin D receptor signaling pathway (GO:0070564; FDR = 0.0069), intrinsic apoptotic signaling in response to DNA damage by p53-class mediator (GO:0042771; FDR = 0.0035), negative regulation of canonical Wnt signaling pathway (GO:0090090; FDR = 0.0118), transforming growth factor beta receptor superfamily signaling pathway (GO:0141091; FDR = 0.0216), response to decreased oxygen levels (GO:0036293; FDR = 0.0176), and response to growth factor (GO:0070848; FDR = 0.0214) (Table S9).

Histone modifications

Using HaploReg v4.2, UF-associated SNPs were annotated for regulatory potential, identifying characteristic histone modification patterns in blood cells, vessels, adipose tissue, and ovaries (Table 7).

The genomic regions of SNPs rs11031731 (*THEM7P, WT1*), rs641760 (*PITPNM2*), rs2553772 (*LOC105376626*), and rs1986649 (*FOXO1*) were marked by characteristic histone modifications in blood cells, including mono-methylation (H3K4me1) and tri-methylation (H3K4me3) at the fourth lysine residue of histone H3, along with acetylation at the 27th (H3K27ac) and 9th (H3K9ac) lysine residues of histone H3. Similarly, SNP rs2553772 (*LOC105376626*) is associated with histone marks in blood vessels; SNPs rs11031731 (*THEM7P, WT1*) and rs1986649 (*FOXO1*) are associated with histone marks in ovaries; and SNPs rs641760 (*PITPNM2*), rs2553772 (*LOC105376626*), and rs1986649 (*FOXO1*) are linked with histone marks in adipose tissue (Table 7).

Computational analysis of UF GWAS SNPs and associated clinical manifestations

Cross-referencing with the RSKP bioinformatics resource revealed population-wide consistency for the identified UF-associated SNPs. The risk variants rs11031731 (*THEM7P/WT1*), rs641760 (*PITPNM2*), rs2553772 (*LOC105376626*), and rs1986649 (*FOXO1*) demonstrated conserved risk-increasing effects across ethnic groups, while rs66998222 (*LOC102723323*) maintained its protective association. These directional effects extended to both UF susceptibility and heavy menstrual bleeding phenotypes in diverse populations. Additionally, SNPs were linked with the following UF-related phenotypes: decreased age of menarche (rs1986649 *FOXO1),* increased age of menarche (rs66998222 *LOC102723323* and *rs641760 PITPNM2)*, increased age at natural menopause (rs641760 *PITPNM2* and rs1986649 *FOXO1*), decreased age at natural menopause (rs11031731 *THEM7P, WT1*), increased BMI (rs11031731 *THEM7P, WT1*), and decreased BMI (rs66998222 *LOC102723323* and rs1986649 *FOXO1*) (Table S10).

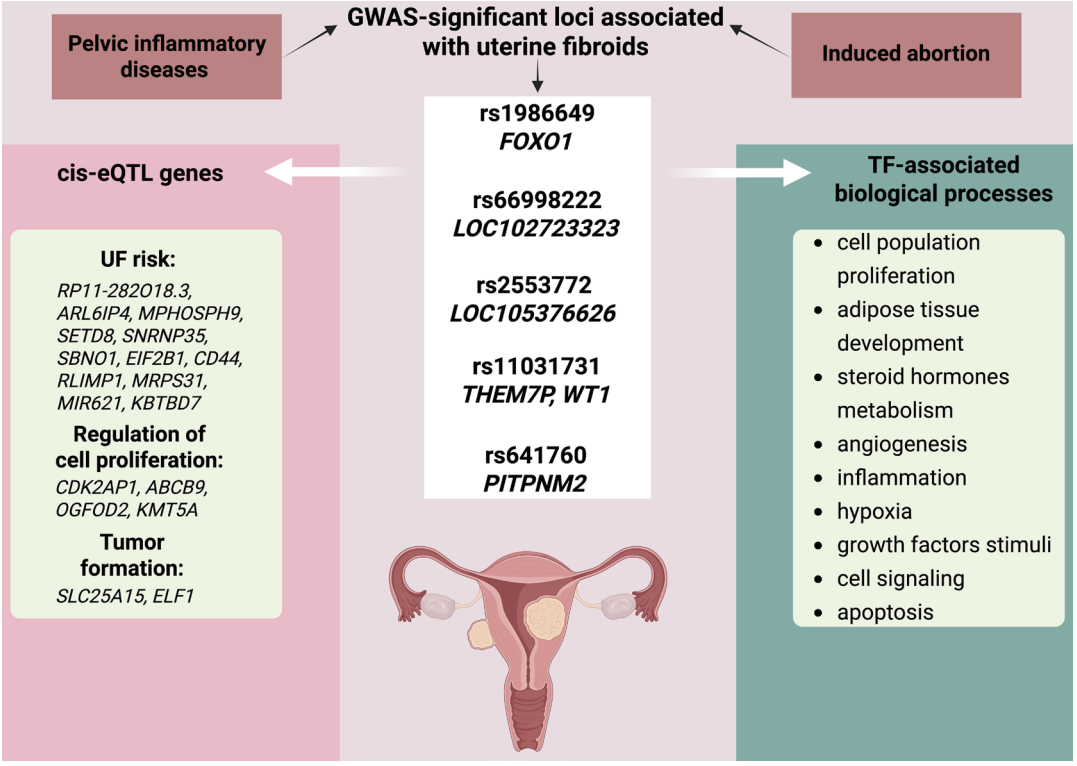

Fig. 5. Bioinformatically predicted biological effects of GWAS loci on UF risk. cis-eQTL, expression quantitative trait loci; TF, transcription factor; UF, uterine fibroid; GWAS, genome-wide association studies.

Discussion

UF pathogenesis involves a complex interplay between genetic predisposition and environmental factors.[4] Examining how these interactions influence disease onset is critical.[28,29] Among these, induced abortions and PID may act as modulators, influencing both the development and clinical course of UFs.[14,19,30,31] While GWAS have identified numerous susceptibility loci,[9,10,8,32] their interaction with environmental exposures remains understudied. Building on our prior work with this Central Russian cohort, where we demonstrated broad modification of UF-associated loci by reproductive factors,[19] we now extend this paradigm through functional analysis of ten newly selected SNPs, specifically probing abortion- and inflammation-related modulation mechanisms.

We found that abortions and pelvic inflammation may contribute to UFs through three shared biological pathways: 1) disruption of hormonal balance following pregnancy termination, leading to unopposed estrogenic stimulation[33,34]; 2) altered myometrial healing, promoting fibroproliferative activity[35,36]; and 3) increased local inflammation, stimulating cytokine-driven growth pathways (e.g., IL-6, transforming growth factor-β).[37] These factors can potentiate or mitigate genetic predispositions, depending on the locus involved (Fig. 5).

We identified a protective association of rs66998222 and rs641760 in women with a history of induced abortion. Prior GWAS linked rs66998222 (*LOC102723323*) with decreased UF risk,[32] and our data confirm this in both the entire group and abortion-positive patients. Functional analysis revealed that the protective allele A at rs66998222 (*LOC102723323*) enhances binding of TFs involved in negative regulation of proliferation and cytokine responses, particularly relevant in an inflammatory microenvironment (GO:0008285, GO:0071345).[13]

The rs641760 (*PITPNM2*) locus, also protective in this subgroup, modulates the expression of genes such as *CDK2AP1, ABCB9*, and *KMT5A*, which are involved in progesterone-regulated uterine cell growth and tumor regulation, respectively.[38–40] Other target genes include *ARL6IP4* and *MPHOSPH9*, both of which influence estrogen signaling, metabolism, and mTOR activation—processes amplified during hormonal fluctuations post-abortion.[41] Bioinformatic analysis via the RSKP portal confirmed the protective effect of the T allele of rs641760 (*PITPNM2*) and the A allele of rs66998222 (*LOC102723323*) against UFs and heavy menstrual bleeding, as well as their impact on UF-associated phenotypes such as BMI, age at menarche, and age at menopause.

The rs11031731 locus conferred elevated UF risk in the general cohort and the abortion-positive subgroup, but not in patients with PID. This disparity may reflect the dominant role of chronic inflammation in the PID group, overshadowing the genetic effect.[12] Conversely, in patients with a history of induced abortions, the increased UF risk appears to result from the combined effects of inflammation and abrupt changes in steroid sex hormone levels following the procedure. Early termination of pregnancy fails to suppress the tumor-stimulating effects of estrogen during later stages of pregnancy,[14] which can subsequently drive UF growth through various genetic and signaling pathways.[33,34] Functionally, the risk allele A creates TF binding sites that upregulate pathways related to adipogenesis and proliferation (GO:1904177, GO:0008283). These mechanisms are amplified in patients with higher BMI or estrogen exposure, explaining the heightened risk in specific environmental contexts.[42] According to the RSKP portal, this allele increases the risk of not only UF but also elevated BMI,

an important UF risk factor.[4]

This locus demonstrated a protective effect in patients without a history of abortion. This protective effect may stem from the SNP's role in regulating tissue healing and restoration.[35,36] Functional annotation showed that the T allele influences CD44 expression, a gene implicated in tissue remodeling.[43] The SNP also promotes TF binding linked to vascular growth, angiogenesis (GO:0010575, GO:0045766, GO:0001525), and myometrial homeostasis (GO:0042127, GO:0007515), potentially buffering against fibrotic changes in hormonally stable or low-inflammation environments. In patients without a history of induced abortions, this allele may facilitate balanced healing processes, contrasting with the more chaotic cellular responses triggered by injury or inflammation.[36] This ability to regulate tissue repair and maintain homeostasis reduces UF risk by preventing hyperplastic changes in the myometrium.[35]

Although not modulated by abortion or PID, the TT genotype of rs1986649 (*FOXO1*) was associated with earlier onset and accelerated UF growth. *FOXO1* has long been studied as a key gene associated with UF development.[44–46] *FOXO1* regulates progesterone (P4) signaling and inflammatory pathways, such as COX-2 and IL-6, linking endocrine and immune mechanisms.[11,47] eQTL data indicate that it influences the expression of *MRPS31* (p53 interaction),[48] *ELF1* (increased tumor risk),[49] *KBTBD7* (MAPK/AP-1 inflammation),[50] *SLC25A15* (tumor formation under hypoxic conditions),[51] and other genes implicated in tumor metabolism and UF risk. The risk allele T upregulates transforming growth factor-β/SMAD (GO:0071636, GO:0060395, GO:0071560, GO:0017015), SREBP (GO:0032933), and inflammatory IL-4/IL-5 (GO:0032674, GO:0032753) pathways, driving fibrosis and proliferation.[35,52–54] According to the RSKP portal, the SNP rs1986649 (*FOXO1*) is associated with higher UF risk, heavy menstrual bleeding, increased age at natural menopause, and earlier age at menarche, extending the duration of reproductive years and thereby elevating UF risk.[55]

This study has several limitations. First, the limited number of analyzed SNPs may have reduced detectable genetic associations. Second, TaqMan genotyping constraints excluded some SNPs due to probe design issues. Third, the lack of an independent Russian cohort prevented replication analysis. Fourth, the binary classification of induced abortions (present/absent) precluded analysis of procedure frequency effects on genetic risk modulation.

Conclusions

Our findings support a model in which environmental exposures, such as abortion and PID, modulate the penetrance and directionality of GWAS-identified UF loci. Some SNPs exhibit context-specific protective or deleterious effects, likely mediated through hormone-sensitive transcriptional programs and immune pathways. Future work should explore these interactions longitudinally and in multi-ethnic cohorts to inform personalized risk stratification.

Acknowledgments

We gratefully acknowledge the Bioinformatics of Genome Regulation and Structure/Systems Biology conference organizers and reviewers for making this special issue possible.

Funding

This research received no external funding.

Conflict of interest

The authors report that there are no competing interests to declare.

Author contributions

Study design (OB), experiment performance (LP, EB, AD), data analysis (LP, KK, OB), writing of the manuscript (LP, OB). All authors contributed to editorial changes in the manuscript and read and approved the final version.

Ethical statement

The studies involving humans were approved by the Ethical Review Committee of Kursk State Medical University (Protocol №5, May 11, 2021). The studies were conducted in accordance with the guidelines of the Declaration of Helsinki (as revised in 2024), local legislation, and institutional requirements. All participants, or their families/legal guardians, provided written informed consent before enrollment in this study.

Data sharing statement

All data supporting the findings of this study are available within the paper and its Supplementary Information.

References

[1] Giuliani E, As-Sanie S, Marsh EE. Epidemiology and management of uterine fibroids. Int J Gynaecol Obstet 2020;149(1):3–9. doi:10.1002/ijgo.13102, PMID:31960950.

[2] Lou Z, Huang Y, Li S, Luo Z, Li C, Chu K, *et al*. Global, regional, and national time trends in incidence, prevalence, years lived with disability for uterine fibroids, 1990-2019: an age-period-cohort analysis for the global burden of disease 2019 study. BMC Public Health 2023;23(1):916. doi:10.1186/s12889-023-15765-x, PMID:37208621.

[3] Ahmad A, Kumar M, Bhoi NR, Badruddeen, Akhtar J, Khan MI, *et al*. Diagnosis and management of uterine fibroids: current trends and future strategies. J Basic Clin Physiol Pharmacol 2023;34(3):291–310. doi:10.1515/jbcpp-2022-0219, PMID:36989026.

[4] Pavone D, Clemenza S, Sorbi F, Fambrini M, Petraglia F. Epidemiology and Risk Factors of Uterine Fibroids. Best Pract Res Clin Obstet Gynaecol 2018;46:3–11. doi:10.1016/j.bpobgyn.2017.09.004, PMID:29054502.

[5] Lazarenko V, Churilin M, Azarova I, Klyosova E, Bykanova M, Ob'edkova N, *et al*. Comprehensive Statistical and Bioinformatics Analysis in the Deciphering of Putative Mechanisms by Which Lipid-Associated GWAS Loci Contribute to Coronary Artery Disease. Biomedicines 2022;10(2):259. doi:10.3390/biomedicines10020259, PMID:35203469.

[6] Loktionov AV, Kobzeva KA, Karpenko AR, Sergeeva VA, Orlov YL, Bushueva OY. GWAS-significant loci and severe COVID-19: analysis of associations, link with thromboinflammation syndrome, gene-gene, and gene-environmental interactions. Front Genet 2024;15:1434681. doi:10.3389/fgene.2024.1434681, PMID:39175753.

[7] Omidiran O, Patel A, Usman S, Mhatre I, Abdelhalim H, DeGroat W, *et al*. GWAS advancements to investigate disease associations and biological mechanisms. Clin Transl Discov 2024;4(3):e296. doi:10.1002/ctd2.296, PMID:38737752.

[8] Aissani B, Zhang K, Wiener H. Evaluation of GWAS candidate susceptibility loci for uterine leiomyoma in the multi-ethnic NIEHS uterine fibroid study. Front Genet 2015;6:241. doi:10.3389/fgene.2015.00241, PMID:26236334.

[9] Gallagher CS, Mäkinen N, Harris HR, Rahmioglu N, Uimari O, Cook JP, *et al*. Genome-wide association and epidemiological analyses reveal common genetic origins between uterine leiomyomata and endo-

metriosis. Nat Commun 2019;10(1):4857. doi:10.1038/s41467-019-12536-4, PMID:31649266.
[10] Sakai K, Tanikawa C, Hirasawa A, Chiyoda T, Yamagami W, Kataoka F, *et al*. Identification of a novel uterine leiomyoma GWAS locus in a Japanese population. Sci Rep 2020;10(1):1197. doi:10.1038/s41598-020-58066-8, PMID:31988393.
[11] Szucio W, Bernaczyk P, Ponikwicka-Tyszko D, Milewska G, Pawelczyk A, Wołczyński S, *et al*. Progesterone signaling in uterine leiomyoma biology: Implications for potential targeted therapy. Adv Med Sci 2024;69(1):21–28. doi:10.1016/j.advms.2024.01.001, PMID:38278085.
[12] Kabodmehri R, Etezadi A, Sharami SH, Ghanaei MM, Hosseinzadeh F, Heirati SFD, *et al*. The association between chronic endometritis and uterine fibroids. J Family Med Prim Care 2022;11(2):653–659. doi:10.4103/jfmpc.jfmpc_1470_21, PMID:35360819.
[13] Roncari D, Politch JA, Sonalkar S, Finneseth M, Borgatta L. Inflammation or infection at the time of second trimester induced abortion. Contraception 2013;87(1):67–70. doi:10.1016/j.contraception.2012.09.016, PMID:23102591.
[14] Song L, Shen L, Mandiwa C, Yang S, Liang Y, Yuan J, *et al*. Induced and Spontaneous Abortion and Risk of Uterine Fibroids. J Womens Health (Larchmt) 2017;26(1):76–82. doi:10.1089/jwh.2016.5913, PMID:27632700.
[15] Stoicescu M, Bungău SG, Ţiţ DM, Muţiu G, Purza AL, Iovan VC, *et al*. Carcinogenic uterine risk of repeated abortions: hormone receptors tumoral expression. Rom J Morphol Embryol 2017;58(4):1429–1434. PMID:29556637.
[16] Doulgeraki T, Papageorgopoulou M, Iliodromiti S. The genetic background of female reproductive disorders: a systematic review. Curr Opin Obstet Gynecol 2023;35(5):426–433. doi:10.1097/GCO.0000000000000896, PMID:37266690.
[17] Golovchenko OV. Features of interlocus interactions in the formation of isolated and combined pregnancy complications. Res Results Biomed 2024;10(4):532–552. doi:10.18413/2658-6533-2024-10-4-0-4.
[18] Buyukcelebi K, Duval AJ, Abdula F, Elkafas H, Seker-Polat F, Adli M. Integrating leiomyoma genetics, epigenomics, and single-cell transcriptomics reveals causal genetic variants, genes, and cell types. Nat Commun 2024;15(1):1169. doi:10.1038/s41467-024-45382-0, PMID:38326302.
[19] Ponomareva L, Kobzeva K, Bushueva O. GWAS-Significant Loci and Uterine Fibroids Risk: Analysis of Associations, Gene-Gene and Gene-Environmental Interactions. Front Biosci (Schol Ed) 2024;16(4):24. doi:10.31083/j.fbs1604024, PMID:39736018.
[20] Huang D, Magaoay B, Rosen MP, Cedars MI. Presence of Fibroids on Transvaginal Ultrasonography in a Community-Based, Diverse Cohort of 996 Reproductive-Age Female Participants. JAMA Netw Open 2023;6(5):e2312701. doi:10.1001/jamanetworkopen.2023.12701, PMID:37163265.
[21] Wesselink AK, Wegienka G, Coleman CM, Geller RJ, Harmon QE, Upson K, *et al*. A prospective ultrasound study of cigarette smoking and uterine leiomyomata incidence and growth. Am J Obstet Gynecol 2023;229(2):151.e1–151.e8. doi:10.1016/j.ajog.2023.04.041, PMID:37148957.
[22] Koressaar T, Remm M. Enhancements and modifications of primer design program Primer3. Bioinformatics 2007;23(10):1289–1291. doi:10.1093/bioinformatics/btm091, PMID:17379693.
[23] Calle ML, Urrea V, Malats N, Van Steen K. mbmdr: an R package for exploring gene-gene interactions associated with binary or quantitative traits. Bioinformatics 2010;26(17):2198–2199. doi:10.1093/bioinformatics/btq352, PMID:20595460.
[24] Shilenok I, Kobzeva K, Soldatov V, Deykin A, Bushueva O. C11orf58 (Hero20) Gene Polymorphism: Contribution to Ischemic Stroke Risk and Interactions with Other Heat-Resistant Obscure Chaperones. Biomedicines 2024;12(11):2603. doi:10.3390/biomedicines12112603, PMID:39595169.
[25] Belykh AE, Soldatov VO, Stetskaya TA, Kobzeva KA, Soldatova MO, Polonikov AV, *et al*. Polymorphism of SERF2, the gene encoding a heat-resistant obscure (Hero) protein with chaperone activity, is a novel link in ischemic stroke. IBRO Neurosci Rep 2023;14:453–461. doi:10.1016/j.ibneur.2023.05.004, PMID:37252629.
[26] Kobzeva KA, Shilenok IV, Belykh AE, Gurtovoy DE, Bobyleva LA, Krapiva AB, *et al*. C9orf16 (BBLN) gene, encoding a member of Hero proteins, is a novel marker in ischemic stroke risk. Res Results Biomed 2022;8(3):278–292. doi:10.18413/2658-6533-2022-8-3-0-2.
[27] Shilenok I, Kobzeva K, Stetskaya T, Freidin M, Soldatova M, Deykin A, *et al*. SERPINE1 mRNA Binding Protein 1 Is Associated with Ischemic Stroke Risk: A Comprehensive Molecular-Genetic and Bioinformatics Analysis of SERBP1 SNPs. Int J Mol Sci 2023;24(10):8716. doi:10.3390/ijms24108716, PMID:37240062.
[28] Shilenok I, Kobzeva K, Deykin A, Pokrovsky V, Patrakhanov E, Bushueva O. Obesity and Environmental Risk Factors Significantly Modify the Association between Ischemic Stroke and the Hero Chaperone C19orf53. Life (Basel) 2024;14(9):1158. doi:10.3390/life14091158, PMID:39337941.
[29] Stetskaya TA, Kobzeva KA, Zaytsev SM, Shilenok IV, Komkova GV, Goryainova NV, *et al*. HSPD1 gene polymorphism is associated with an increased risk of ischemic stroke in smokers. Res Results Biomed 2024;10(2):175–186. doi:10.18413/2658-6533-2024-10-2-0-1.
[30] AlAshqar A, Reschke L, Kirschen GW, Borahay MA. Role of inflammation in benign gynecologic disorders: from pathogenesis to novel therapies†. Biol Reprod 2021;105(1):7–31. doi:10.1093/biolre/ioab054, PMID:33739368.
[31] Mikhailiuk IP, Shandanovina YA, Ramazanova DG, Brynza AA, Dzhalaeva KS, Abdulaeva RS, *et al*. Uterine Fibroid in Combination with Adenomyosis. Purulent-Inflammatory Diseases of the Female Genital Organs and Their Effect on Reproductive Function. International transaction journal of engineering, management, and applied sciences and technologies. Abbreviation: Int. Transact. J Eng Manage Appl Sci Tech 2022;13(11):13A11J:1-9. doi:10.14456/ITJEMAST.2022.220.
[32] Kim J, Williams A, Noh H, Jasper EA, Jones SH, Jaworski JA, *et al*. Genome-wide meta-analysis identifies novel risk loci for uterine fibroids within and across multiple ancestry groups. Nat Commun 2025;16(1):2273. doi:10.1038/s41467-025-57483-5, PMID:40050615.
[33] Borahay MA, Asoglu MR, Mas A, Adam S, Kilic GS, Al-Hendy A. Estrogen Receptors and Signaling in Fibroids: Role in Pathobiology and Therapeutic Implications. Reprod Sci 2017;24(9):1235–1244. doi:10.1177/1933719116678686, PMID:27872195.
[34] Reis FM, Bloise E, Ortiga-Carvalho TM. Hormones and pathogenesis of uterine fibroids. Best Pract Res Clin Obstet Gynaecol 2016;34:13–24. doi:10.1016/j.bpobgyn.2015.11.015, PMID:26725037.
[35] Hampton G, Kim J, Edwards TL, Hellwege JN, Velez Edwards DR. Uterine leiomyomata and keloids fibrosis origins: a mini-review of fibroproliferative diseases. Am J Physiol Cell Physiol 2023;325(4):C817–C822. doi:10.1152/ajpcell.00181.2023, PMID:37642233.
[36] Roeder HA, Cramer SF, Leppert PC. A look at uterine wound healing through a histopathological study of uterine scars. Reprod Sci 2012;19(5):463–473. doi:10.1177/1933719111426603, PMID:22344737.
[37] Protic O, Toti P, Islam MS, Occhini R, Giannubilo SR, Catherino WH, *et al*. Possible involvement of inflammatory/reparative processes in the development of uterine fibroids. Cell Tissue Res 2016;364(2):415–427. doi:10.1007/s00441-015-2324-3, PMID:26613601.
[38] Cheon YP, Kim CH. Progesterone is primary regulator of Cdk2ap1 gene expression and tissue-specific expression in the uterus. J Endocrinol Invest 2010;33(9):650–656. doi:10.1007/BF03346665, PMID:20354353.
[39] Dai Y, Liu X, Zhu Y, Mao S, Yang J, Zhu L. Exploring Potential Causal Genes for Uterine Leiomyomas: A Summary Data-Based Mendelian Randomization and FUMA Analysis. Front Genet 2022;13:890007. doi:10.3389/fgene.2022.890007, PMID:35903355.
[40] Kukita A, Sone K, Kaneko S, Kawakami E, Oki S, Kojima M, *et al*. The Histone Methyltransferase SETD8 Regulates the Expression of Tumor Suppressor Genes via H4K20 Methylation and the p53 Signaling Pathway in Endometrial Cancer Cells. Cancers (Basel) 2022;14(21):5367. doi:10.3390/cancers14215367, PMID:36358786.
[41] Xu LL, Shang Y, Qu XN, He HM. M-Phase Phosphoprotein 9 upregulation associates with poor prognosis and activates mTOR signaling in gastric cancer. Kaohsiung J Med Sci 2021;37(3):208–214. doi:10.1002/kjm2.12319, PMID:33174370.
[42] Bhardwaj P, Au CC, Benito-Martin A, Ladumor H, Oshchepkova S, Moges R, *et al*. Estrogens and breast cancer: Mechanisms involved in obesity-related development, growth and progression. J Steroid Bio-

chem Mol Biol 2019;189:161–170. doi:10.1016/j.jsbmb.2019.03.002, PMID:30851382.
[43] Sun YH, Wang CM, Shen HP, Lee CY, Lin CW, Yang SF, *et al*. Impact of CD44 genetic variants on clinicopathological characteristics of uterine cervical cancer patients. Int J Med Sci 2024;21(8):1428–1437. doi:10.7150/ijms.96414, PMID:38903932.
[44] Fedotova M, Barysheva E, Bushueva O. Pathways of Hypoxia-Inducible Factor (HIF) in the Orchestration of Uterine Fibroids Development. Life (Basel) 2023;13(8):1740. doi:10.3390/life13081740, PMID:37629598.
[45] Omar M, Laknaur A, Al-Hendy A, Yang Q. Myometrial progesterone hyper-responsiveness associated with increased risk of human uterine fibroids. BMC Womens Health 2019;19(1):92. doi:10.1186/s12905-019-0795-1, PMID:31288815.
[46] Välimäki N, Kuisma H, Pasanen A, Heikinheimo O, Sjöberg J, Bützow R, *et al*. Genetic predisposition to uterine leiomyoma is determined by loci for genitourinary development and genome stability. Elife 2018;7:e37110. doi:10.7554/eLife.37110, PMID:30226466.
[47] Lappas M. Forkhead box O1 (FOXO1) in pregnant human myometrial cells: a role as a pro-inflammatory mediator in human parturition. J Reprod Immunol 2013;99(1-2):24–32. doi:10.1016/j.jri.2013.04.005, PMID:23778262.
[48] Revathi Paramasivam O, Gopisetty G, Subramani J, Thangarajan R. Expression and affinity purification of recombinant mammalian mitochondrial ribosomal small subunit (MRPS) proteins and protein-protein interaction analysis indicate putative role in tumourigenic cellular processes. J Biochem 2021;169(6):675–692. doi:10.1093/jb/mvab004, PMID:34492114.
[49] Leo PJ, Madeleine MM, Wang S, Schwartz SM, Newell F, Pettersson-Kymmer U, *et al*. Defining the genetic susceptibility to cervical neoplasia-A genome-wide association study. PLoS Genet 2017;13(8):e1006866. doi:10.1371/journal.pgen.1006866, PMID:28806749.
[50] Kim G, Jang G, Song J, Kim D, Lee S, Joo JWJ, *et al*. A transcriptome-wide association study of uterine fibroids to identify potential genetic markers and toxic chemicals. PLoS One 2022;17(9):e0274879. doi:10.1371/journal.pone.0274879, PMID:36174000.
[51] Zhang Q, Wei T, Jin W, Yan L, Shi L, Zhu S, *et al*. Deficiency in SLC25A15, a hypoxia-responsive gene, promotes hepatocellular carcinoma by reprogramming glutamine metabolism. J Hepatol 2024;80(2):293–308. doi:10.1016/j.jhep.2023.10.024, PMID:38450598.
[52] Ciebiera M, Włodarczyk M, Wrzosek M, Męczekalski B, Nowicka G, Łukaszuk K, *et al*. Role of Transforming Growth Factor β in Uterine Fibroid Biology. Int J Mol Sci 2017;18(11):2435. doi:10.3390/ijms18112435, PMID:29149020.
[53] Konenkov VI, Koroleva EG, Orlov NB, Prokof'ev VF, Shevchenko AV, Novikov AM, *et al*. Anti-inflammatory activity of serum cytokines (IL-4, IL-10, IL-13) and the natural IL-1β receptor antagonist (IL-1Ra) in women with uterine myoma. Obstet Gynecol 2018;10:80–85. doi:10.18565/aig.2018.10.80-85.
[54] Zhao H, Wu L, Yan G, Chen Y, Zhou M, Wu Y, *et al*. Inflammation and tumor progression: signaling pathways and targeted intervention. Signal Transduct Target Ther 2021;6(1):263. doi:10.1038/s41392-021-00658-5, PMID:34248142.
[55] Wise LA, Laughlin-Tommaso SK. Epidemiology of Uterine Fibroids: From Menarche to Menopause. Clin Obstet Gynecol 2016;59(1):2–24. doi:10.1097/GRF.0000000000000164, PMID:26744813.